



## The mesoscale variability in the Caribbean Sea. Part II: Energy sources

Julien Jouanno<sup>a,\*</sup>, Julio Sheinbaum<sup>a</sup>, Bernard Barnier<sup>b</sup>, Jean-Marc Molines<sup>b</sup>

<sup>a</sup>Departamento de Oceanografía Física, CICESE, Km. 107 Carretera Tijuana-Ensenada, Ensenada, C.P. 22860 Baja California, Mexico

<sup>b</sup>MEOM, LEGI-CNRS, BP53, 38041, Grenoble Cedex 9, France

### ARTICLE INFO

#### Article history:

Received 2 April 2008

Received in revised form 19 October 2008

Accepted 23 October 2008

Available online 12 November 2008

#### Keywords:

Caribbean

Ocean model

Embedding

Mesoscale eddies

Instability

### ABSTRACT

The processes which drive the production and the growth of the strong mesoscale eddy field in the Caribbean Sea are examined using a general circulation model. Diagnostics of the simulations suggest that:

(1) The mean currents in the Caribbean Sea are intrinsically unstable. The nature of the instability and its strength vary spatially due to strong differences of current structure among basins.

(2) The greatest and most energetic eddies of the Caribbean Sea originate in the Venezuela Basin by mixed barotropic-baroclinic instability of an intense jet, formed with waters mostly from the surface return flow of the Meridional Overturning Circulation and the North Equatorial Current which converge and accelerate through the Grenada Passage. The vertical shear of this inflow is enhanced by an eastward undercurrent, which flows along the south American Coast between 100 and 250 m depth. The shallow eddies (less than 200 m depth) formed in the vicinity of the Grenada Passage get rapidly deeper (down to 1000 m depth) and stronger by their interaction with the deep interior flow of the Subtropical Gyre, which enters through passages north of St. Lucia. These main eastern Caribbean inflows merge and form the southern Caribbean Current, whose baroclinic instability is responsible for the westward growth and strengthening of these eddies from the Venezuela to the Colombia Basin.

(3) Eddies of lesser strength are produced in other regions of the Caribbean Sea. Their generation and growth is also linked with instability of the local currents. First, cyclones are formed in the cyclonic shear of the northern Caribbean Current, but appear to be rapidly dissipated or absorbed by the large anticyclones coming from the southern Caribbean. Second, eddies in the Cayman Sea, which impact the Yucatan region, are locally produced and enhanced by barotropic instability of the deep Cayman Current.

(4) The role of the North Brazil Current (NBC) rings is mostly to act as a finite perturbation for the instability of the mean flow. Their presence near the Lesser Antilles is ubiquitous and they appear to be linked with most of the Caribbean eddies. There are some evidences that the frequency at which they form near the Grenada Passage is influenced by the frequency at which the NBC rings impinge the Lesser Antilles. But large Caribbean eddies also form without a close influence of any ring, and comparison between simulations shows that mean eddy kinetic energy and eddy population in the Caribbean Sea are not substantially different in absence or presence of NBC rings: their presence is not a necessary condition for the generation and growth of the Caribbean eddies.

© 2008 Elsevier Ltd. All rights reserved.

### 1. Introduction

Previous observations based and model based studies did not permit to draw a clear view of which processes set the characteristics of the eddy field in the Caribbean Sea, but rather showed several points of controversy. The reason is perhaps that many processes can potentially drive the variability and explain the enhanced eddy production in the region. There is neither a general agreement on whether the energetic eddies originate from local processes such as windstress, current instability or topographic

effects or from remote processes such as propagation of Atlantic Rossby waves or advection of North Brazil Current (NBC) rings.

Among the local processes, the presence of a strong mean wind-stress curl (WSC, see Fig. 2) in the Central Caribbean has been proposed to be a source of energy for the Caribbean mesoscale activity. A model study which excludes incoming perturbations from the Atlantic shows eddies produced southwest of Hispaniola (Oey et al., 2003). The authors suggest that the local mean WSC is responsible for this generation, although they admit that the instability of the Caribbean Current could be inadequately simulated in their experiments. Andrade and Barton (2000) associate the enhancement of eddy activity in the central Caribbean during July–October with the maximum curl of the North Trade Wind during this period. However they do not consider the influence of NBC

\* Corresponding author. Tel.: +52 (646) 1750500.  
E-mail address: [jouanno@cicese.mx](mailto:jouanno@cicese.mx) (J. Jouanno).

rings and that the mean Caribbean Current may also have annual variability correlated with eddy production. Recent observations suggest local wind generation is not enough to explain the eddies vertical structure. The real eddies observed by Silander (2005) in the Venezuela Basin are deep and energetic (maximum swirl speed ranged from 0.3 to 0.6 m s<sup>-1</sup>): it is unlikely that pure wind stress curl, which is not particularly strong in the Venezuela Basin, can spin up in just few weeks at these latitudes such energetic eddies reaching more than 1000 m depth. In addition, altimetry data (e.g., Guerrero et al., 2004) show that most of the anticyclones occur in the southern part of the Caribbean Sea where the WSC is mostly cyclonic.

Another local process which can be responsible for eddy generation and growth is the instability of the main Caribbean Current. Conversion from Mean Kinetic Energy (MKE) to Mean Eddy Kinetic Energy (MEKE) has been proposed to contribute to eddy growth (Carton and Chao, 1999) but not demonstrated. Other hypothesis, provided by Andrade and Barton (2000) is that unstable meandering of the Caribbean Current could form some eddies. Richardson (2005) also suggests that instabilities of the anticyclonic shear of Caribbean jets could help the incoming NBC rings vorticity to organize and amplify into energetic eddies. Diagnostics of our simulations discussed below in Section 2 demonstrate that the main Caribbean currents are prone to be unstable and calculations of energy conversion terms between mean flow (mean kinetic energy and mean stratification) and eddies confirm that the two fields exchange energy. Although the eddy field can transfer energy to the mean flow in some particular regions (Yucatan and Nicaraguan coasts), conversions of energy mainly benefit the eddy field. In addition, we noticed a close correspondence between regions of maximum conversion and regions where MEKE increases. Some regions are dominated by barotropic instability (e.g., the Cayman Sea), whereas other regions are dominated by baroclinic instability (Colombia and Venezuela Basins).

Topography and geography of the Caribbean Sea are quite complex (see Fig. 1 in Jouanno et al., 2008) and they might also have some local influence on both growth and decay of the eddy field. The main Caribbean Current (which we refer to here as the southern Caribbean Current, sCC) flows along the continental coast; our simulations show that the shape of the coast line and the narrowness of the Lesser Antilles passages accelerate the current and modify its instability properties. Topography and geography can also dissipate energy and destroy coherent structures. Altimetry data (Andrade and Barton, 2000) and simulations (Carton and Chao, 1999) show that most of the eastern Caribbean eddies seem dissipated by topographic features in the coastal waters of Nicaragua and do not reach the Yucatan Channel. Our simulations suggest that the strong decrease of MEKE along the Nicaraguan coast in association with an acceleration of the mean flow through the narrow Chibcha Channel allows the Cayman Basin to develop variability with its own particular characteristics.

Concerning a possible remote origin of the variability, the process most often proposed in the literature is the advection of NBC rings through the Lesser Antilles. They originate in the equator, where the reflection of long Rossby waves on the Brazilian coast generates a cyclonic-anticyclonic system which travels northward along this coast. Nonlinear interactions with the coast and the  $\beta$ -effect contribute to the growth of anticyclonic eddies (Jochum and Rizzoli, 2003) which can reach the narrow and shallow passages of the Lesser Antilles (Fratantoni et al., 1995). Carton and Chao (1999) suggest that the interaction of the incoming NBC rings with the topography around the Island of Trinidad and Tobago, results in pairs of cyclones anticyclones which become part and interact with the Caribbean Current. Murphy et al. (1999) also invoke the NBC retroflection and suggest that potential vorticity (PV) of the NBC rings is advected through the Lesser Antilles,

and acts as finite amplitude perturbations for mixed barotropic and internal mode baroclinic instabilities which result in meso-scale features. Analyzing drifter data, Richardson (2005) proposes that anticyclones in the Venezuela Basin could originate with the vorticity advected by the NBC rings, hypothesis consistent with process studies on eddy flux through islands chains (Simmons and Nof, 2002; Tanabe and Cenedese, 2008). Nevertheless, drifters show few direct evidences of rings entering completely. Another process study demonstrates that Atlantic Rossby Waves can pass through ocean barriers such as the Lesser Antilles (Pedlosky, 2000).

Recently, Chérubin and Richardson (2007) proposed a link between the number of eddies in the eastern Caribbean, inferred from drifters, and the presence of the fresh water plume, which would enhance the potential vorticity gradients during August–December. It is interesting to contrast their results with surface geostrophic velocity anomalies derived from 15 years of altimetry data (AVISO). They indicate that the maximum of eddy energy in the eastern Caribbean occurs during June–July (see Fig. 1). Clearly, it is difficult to relate the arrival of the freshwater plume in the eastern Caribbean during August–December with the local maximum of eddy energy two months before and also use it as the source of energetic eddies all along the year. The arrival of the freshwater plume can certainly impact eddy generation and maintenance (e.g during the period September–November) but given the characteristics of the instability processes in the model and altimetry observations, it is difficult to make it the main source of variability in the eastern Caribbean.

So there is no consensus on what are the energy sources of the Caribbean eddies and questions remain open:

- What is the dominant process in the genesis of the most energetic Caribbean eddies?
- Which processes are responsible for the westward intensification of the eddy energy in the Caribbean Sea?
- What is the real impact of the NBC rings on the Caribbean eddy variability?

The aim of this paper is to try to answer these questions. The different numerical experiments used to solve this problem, as well as the characteristics of the Caribbean mean flow and eddy field, are described in part I of this study (Jouanno et al., 2008). As shown in part I, the most energetic mesoscale variability is embedded or occurs in the sCC, so we mainly focus on this current. We start by analyzing its conditions of instability in Section 2 and by examining in Section 3 the exchange between mean and eddy field along its core. In Section 4 we discuss how the various Carib-

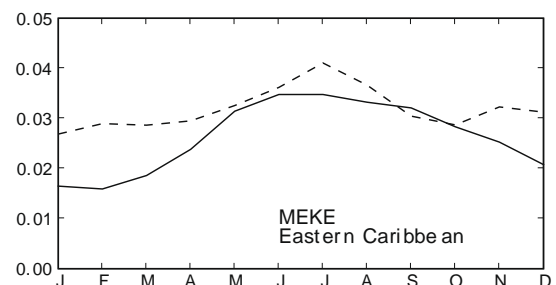


**Fig. 1.** Monthly Mean Eddy Kinetic Energy (MEKE) (m<sup>2</sup> s<sup>-2</sup>) at the surface calculated with 15 years (1992-10-14 to 2007-04-18) of geostrophic velocity anomalies derived from altimetry data (solid line) and 6 years of surface velocity from NOSLIP experiment (see Jouanno et al., 2008). Surface velocities were sorted by month to compute monthly mean velocities. The monthly MEKE is then computed from velocity anomalies with respect to the corresponding monthly mean velocity. Results are averaged over the area 62–70°W, 11–18°N.

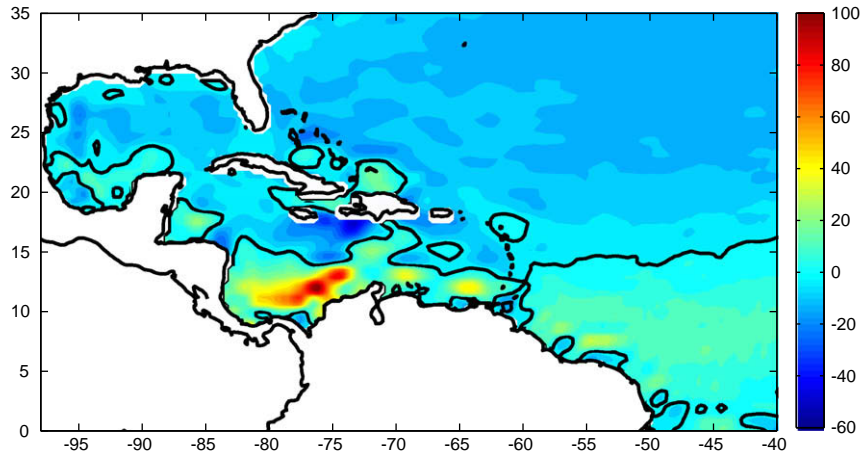


**Fig. 2.** Annual mean WSC ( $10^{-8} \text{ N m}^{-3}$ ) from ERA15 the first “European Center for Medium range Weather Forecasting” ECMWF re-analysis. Null WSC is indicated with black lines. In particular, the continuous zonal line centered around  $15^\circ\text{N}$  indicates a zone known as the ITCZ (Inter Tropical Convergence Zone). In the Caribbean Sea, the annual mean position of the ITCZ separates two local maxima of WSC: a maximum of anticyclonic vorticity, south of Hispaniola, and a maximum of cyclonic vorticity in the southern Colombia Basin.

bean inflows organize into an unstable current. Section 5 details and illustrates the formation process of the most energetic eddies in the eastern Caribbean. Section 6 investigates the importance that NBC rings and Atlantic perturbations could have in setting the characteristics of the Caribbean variability. Section 7 analyzes the dynamics of other regions of eddy production, such as the northern Caribbean Current (nCC), the Panama-Colombia Gyre or the Cayman Current. Finally, Section 8 gives a summary and conclusions.

## 2. Instability conditions of the sCC

The sCC has a strong vertical shear and its flow is narrow and strong, as shown by model (e.g., part I of this study) or observations (Hernández-Guerra and Joyce, 2000). The geographical position, intermediate between the equator and high latitudes, allows the Caribbean Basin to support relatively fast baroclinic and barotropic responses. All these characteristics are favorable to the growth of baroclinic instability particularly for a westward current (Talley, 1983). Strong horizontal shear also occurs and could turn the currents barotropically unstable at their edges. This section studies and quantifies the stability of the sCC in the Venezuela and Colombia Basins, by analyzing outputs from experiment NOSLIP (in part I of this study, several simulation were analyzed and compared with observations, and the experiment NOSLIP resulted to be the more realistic). Note that some characteristics of the different simulations which have been carried out are recalled in Table 1, but for further details the reader is invited to consult part I.

### 2.1. Baroclinic time scale

The correspondence of areas with high variability and areas with a short baroclinic time scale suggests that baroclinicity of large scale flows is related to eddy production (Tréguier et al.,

1997). The baroclinic time scale parameter establishes the temporal scale for the growth of baroclinic waves in the Eady problem:

$$T = \frac{\sqrt{Ri}}{f}, \quad (1)$$

where  $f$  is the Coriolis parameter, and the horizontal bar is the vertical mean.

$$Ri = \frac{N^2}{\left(\frac{\partial U}{\partial z}\right)^2 + \left(\frac{\partial V}{\partial z}\right)^2} \quad (2)$$

is the Richardson number where  $\partial U/\partial z$  and  $\partial V/\partial z$  represent the vertical shear of the mean flow and  $N$  is the mean stratification. The baroclinic time scale (Eq. (1)), averaged from 50 to 400 m depth and calculated from model data (Fig. 3a) is consistent with the one calculated using temperature and salinity data from the Levitus Climatology and the thermal wind equations (Fig. 4): short time scales (from 3 to 10 days) are found in the Caribbean Sea, all along the core of the sCC. Note that in Fig. 4, values are of same order in the sCC core than those found in the Gulf Stream. The mesoscale turbulence around the Gulf Stream is known to be produced by baroclinic instabilities of the current itself. This suggests that the instability of the sCC can have a great impact on the variability of the Caribbean Basin.

In Fig. 3a, the shortest values are localized in the Colombia Basin and north of Maracaibo. In Fig. 3b, the baroclinic time scale is averaged from 30 to 100 m depth. Taking this different interval of depths allows to show that some regions have a very short baroclinic time scale localized in the upper layers, associated with a strong vertical shear in the upper 100 m depth. Two regions have the shortest values. The first one is just west of the Lesser Antilles at  $64^\circ\text{W}$ , where the upper inflow spreads into the Venezuela Basin. A second one occurs at  $72^\circ\text{W}$ , where the sCC is deflected and intensified by geographic effects. In both regions, the mean currents are

**Table 1**

Characteristics of the experiments used in this study. Further details can be found in table 2 of Jouanno et al. (2008).

Name	Horiz. Resol.	Forcings	Partial Steps	Horiz. boundary condition	Special feature
REF	$1/15^\circ$	Daily Clim.	✓	Free slip	
MEAN	$1/15^\circ$	Annual mean	✓	Free slip	
NOSLIP	$1/15^\circ$	Daily Clim.	✓	Noslip	
VISC	$1/15^\circ$	Daily Clim.	✓	Free slip	Laplacian viscosity is added in the NBC region

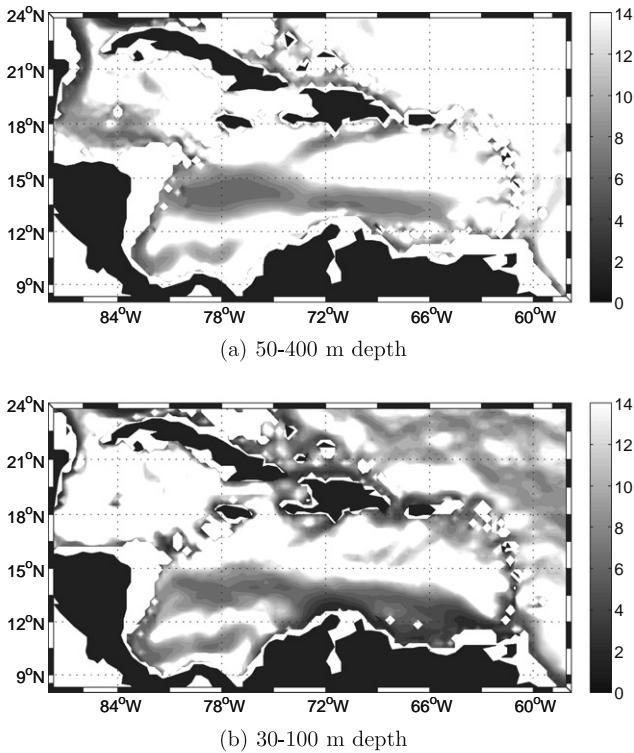


**Fig. 3.** Baroclinic time scale (days) averaged from 50 m depth to 400 m depth (a) and from 30 to 100 m depth (b). Six years of model data from NOSLIP were used. Regions with short baroclinic time scale are regions for which the mean flow can develop baroclinic instability on a short time scale. It means that these regions will be more unstable than regions with an higher baroclinic time scale.

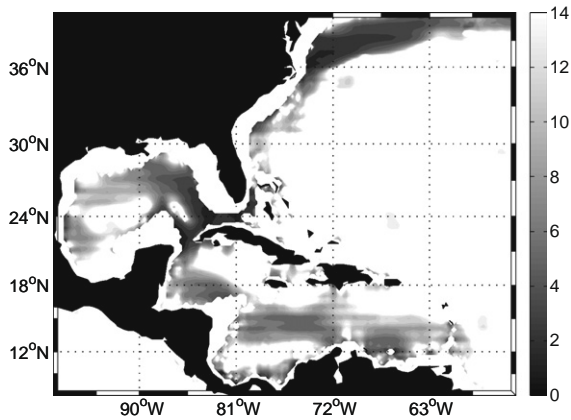


**Fig. 4.** Baroclinic time scale (days) averaged from 50 m depth to 400 m depth and calculated using temperature and salinity data from the Levitus Climatology and the thermal wind equations.

strong (Fig. 5 in part I), and values of MEKE increase westward (see for example the MEKE horizontal field in Fig. 12 of part I).

Using the Eady time-scale to identify instability regions might be too naive but gives some intuition on the dynamical state of the mean currents. We will confirm and quantify the relation between baroclinic instability and MEKE increase on those areas in the following sections.

### 2.2. Necessary conditions for instability

Analysis of the Quasi-Geostrophic (QG) equations shows that a change in sign in the meridional gradient of Potential Vorticity (PV)

of the mean flow is a necessary condition of instability in a stratified ocean (Pedlosky, 1979). QG equations combined with thermal wind equations give, for a zonal flow, the following meridional gradient of Quasi Geostrophic Potential Vorticity (QGPV) which is only a function of depth ( $z$ ) and latitude (or northward direction  $y$ ):

$$Q_y = \beta - U_{yy} + f(\overline{\rho}_y/\overline{\rho}_z)_z, \quad (3)$$

where  $\beta$  is the meridional gradient of planetary vorticity,  $U(y,z)$  the zonal velocity of the mean flow,  $\rho(y,z)$  the density of the water, the overline the time mean and subscripts partial derivative. A vertical change of sign of  $Q_y$  is related to baroclinic instability and horizontal change of sign to barotropic instability.

For any meridional cross section (chosen such as zonal variations of the flow are weak), the necessary condition of instability is satisfied for the main Caribbean currents, although the strength of  $Q_y$  gradients depends on the chosen section. To point out some relevant differences between the Caribbean Basins, we select three sections: “Venezuela” (63°W) is located just west to the Lesser Antilles, “Colombia” (71°W) lies from Maracaibo to Hispaniola and “Cayman” (83°W) from Nicaragua to Cuba. This last one will be analyzed with more details in Section 7.

In the “Venezuela” section, meridional and vertical gradients of  $Q_y$  occur in the core of a shallow westward jet close to the South American Coast (zonal velocity is shown by the contours). This jet is formed mostly by waters from the North Equatorial Current (NEC) and the return flow of the MOC which have been accelerated through Grenada and St. Vincent Passages. On its vertical and horizontal edges,  $Q_y$  changes sign. There the barotropic term ( $\beta - U_{yy}$ , lower panel) is of same order than the stretching term  $f(\overline{\rho}_y/\overline{\rho}_z)_z$ , suggesting a mixed barotropic-baroclinic instability of the jet. For the rest of the section, there are no more strong  $Q_y$  gradients. This is in agreement with the fact that the growth of large anticyclones is mostly localized downstream of the Grenada Passage at 12°N.

For the “Colombia” section (in Fig. 5), the sCC reaches 500 m depth in contrast to the 100 m depth of the coastal jet in the “Venezuela” section. This westward deepening is due to the merging of the “Venezuela” upper coastal flow with intermediate waters from the Subtropical Gyre near 65–14°N as previously described. The energetic core of the current remains shallow, since mean speeds, up to  $0.15 \text{ m s}^{-1}$ , are found only from the surface to 200 m depth. The westward flow seen in the northern part of the section is the nCC, which is deeper and with velocities lower than those in the sCC. The sign of  $Q_y$  changes on the edge of both currents. In the south, between 13°N and 15°N, the change of sign occurs in the vertical for the first time at 50 m depth and two other times roughly at 180 m depth and 300 m depth, due to the presence of an eastward undercurrent close to the coast, the Caribbean Coastal Undercurrent. But it is at 50 m depth (i.e., in the core of the sCC) that  $Q_y$  gradients are stronger. The barotropic term for this section (lower panel) shows a maximum between the eastward current and the core of the sCC but the gradients involved are smaller than the gradients associated with the stretching term (see the top panel) in the upper 100 m depth: vertical shear dominates  $Q_y$ . This is an indication that the baroclinic instability of the sCC prevails over its barotropic instability. This will be confirmed later with analysis of energy conversions.

Although this analysis gives necessary but not sufficient conditions for instability, the different terms are representative of the dynamical state of the mean flow. The coherence between the interpretation of PV gradients and the characteristics of the eddy field indicates this is a useful approach to understand the dynamics. We could demonstrate that conditions for instability of the mean flow are basically matched everywhere in the basin where a mean current is present. However, regions which appear more likely unstable (where we expect the fastest growth of the pertur-

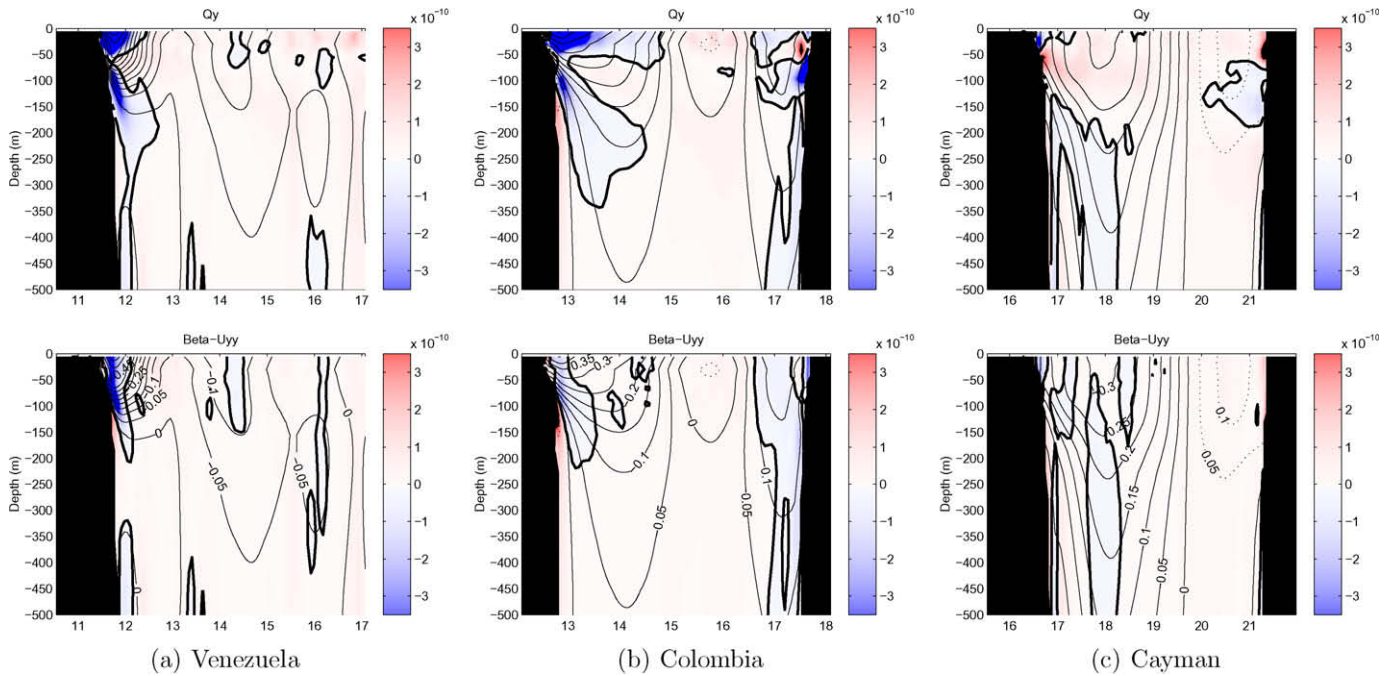


**Fig. 5.** Meridional gradient of Quasi Geostrophic mean potential vorticity  $Q_y$  ( $s^{-1}m^{-1}$ , upper panel) and mean barotropic term  $\beta - U_{yy}$  ( $s^{-1}m^{-1}$ , bottom panel) for three sections: “Venezuela” just west to the Lesser Antilles ( $63^\circ W$ ), “Colombia” from Maracaibo to Hispaniola ( $71^\circ W$ ) and “Cayman” in the Cayman Basin ( $83^\circ W$ ). NOSLIP outputs were used. Contours represent the mean zonal velocity ( $m s^{-1}$ ), with continuous lines as westward velocity and dashed lines as eastward velocity. Bold lines represent null values of  $Q_y$ . A change of sign of  $Q_y$  in the domain is a necessary condition for instability. A vertical (horizontal) change of sign of  $Q_y$  is related to baroclinic (barotropic) instability.

bations) are the jet downstream the Grenada Passage and the core of the sCC. This suggests that Caribbean eddies could be generated and grow all along the sCC from its source at the Grenada passage. To complement this analysis, next section investigates the energy balance and exchanges between mean and eddy field to understand more clearly the dynamical processes leading to the observed model variability.

### 3. Eddy-mean flow interactions in the sCC

Energy analysis gives determining information on the generation of the mesoscale activity by the mean circulation and highlights the strong dynamical differences between different regions of the Venezuela and Colombia Basins. We focus on the interactions between energy components. Effects of advection, forcing or dissipation are not considered here. Following the framework described in Beckmann et al. (1994), the energy transfer terms are given by:

$$(MPE \rightarrow MKE) T_1 = g \iiint \bar{\rho w} dV, \quad (4)$$

$$(MEPE \rightarrow MPE) T_2 = g \iiint \frac{\bar{u} \rho' (\partial \bar{\rho} / \partial x) + \bar{v} \rho' (\partial \bar{\rho} / \partial y)}{d\bar{\rho} / dz} dV, \quad (5)$$

$$(MEKE \rightarrow MEPE) T_3 = -g \iiint \bar{\rho' w} dV, \quad (6)$$

$$(MKE \rightarrow MEKE) T_4 = - \iiint \bar{u' u'} \frac{\partial \bar{u}}{\partial x} + \bar{u' v'} \left( \frac{\partial \bar{v}}{\partial x} + \frac{\partial \bar{u}}{\partial y} \right) + \bar{v' v'} \frac{\partial \bar{v}}{\partial y} dV \quad \text{and} \quad (7)$$

$$(MEKE \rightarrow MKE) T_5 = \iiint \bar{u} \frac{\partial \bar{u' v'}}{\partial x} + \bar{u} \frac{\partial \bar{u' v'}}{\partial y} + \bar{v} \frac{\partial \bar{u' v'}}{\partial x} + \bar{v} \frac{\partial \bar{v' v'}}{\partial y} dV, \quad (8)$$

where the overline is a time mean and the prime represents fluctuations around this mean.  $T_1$  represents the conversion of Mean Kinetic Energy (MKE) into potential energy available in the mean stratification (MPE).  $T_2$  is the conversion between MPE and eddy potential energy (MEPE), and is commonly interpreted as an indication of baroclinic instability when it has negative values. However, baroclinic instability processes also need a transfer of MEPE to MEKE. This transfer is given by  $T_3$  (when  $<0$ ). So, we will associate baroclinic instability processes when  $T_2$  and  $T_3$  are both positive.  $T_4$  represents the energy received by the eddy field from the work of Reynolds stresses between MKE and MEKE. This is not a conversion term in the sense that  $T_4$  does not represent the energy lost by MKE. Such conversion is represented by the term  $-T_5$ . This kind of analysis has been widely carried out (e.g., Masina and Philander, 1999; Jochum and Rizzoli, 2003), but Plumb (1983) and Marinone and Ripa (1984) have shown that care should be exercised in its interpretation. Combined with previous results, their interpretation here shows some consistency.

The regional differences and localized dynamics of the Caribbean Sea lead to focus on regional energy budgets. The different terms ( $T_1$ – $T_5$ ) are integrated over the regions indicated in Fig. 6 from the surface to 1000 m depth. The choice of the regions is driven by their dynamical interest with respect to the mesoscale activity, in particular local increase or decrease of MEKE.

Movies and MEKE maps show that Venezuela and Colombia are regions of eddy production. In the diagrams of Fig. 6, it can be seen that positive values of both  $T_2$  and  $T_3$  are found for Colombia and Venezuela, suggesting occurrence of baroclinic instability in these basins. Barotropic instabilities, represented by positive values of  $T_4$ , are also identified for both Colombia and Venezuela Basins.

It was seen in part I that passing the Chibcha Channel toward the Cayman Sea, the variability of the flow decreases drastically. It was proposed by Andrade and Barton (2000) and Carton and

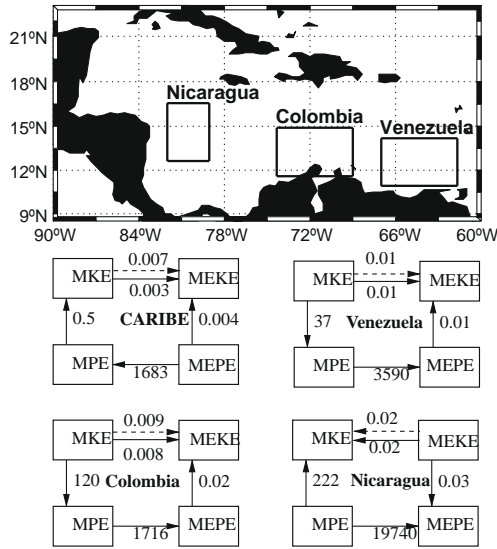


**Fig. 6.** Mean energy interaction terms ( $10^{-7} \text{ m}^{-2} \text{ s}^{-3}$  in the NOSLIP experiment). Terms were averaged over the regions indicated in (a) and from the surface to 1000 m depth. The area CARIBE covers the whole Caribbean Sea and is limited by the continental coast and the chain of the Antilles. Between MKE and MEKE the dashed arrow is  $T_4$  and the continuous arrow is  $T_5$ .

Chao (1999) that eddies in the Colombia Basin are dissipated by topographic features in the coastal waters of Nicaragua. Movies of surface model velocity suggest that eddies are absorbed by the mean flow in this region. This view is confirmed by the energy budget since Fig. 6 shows for “Nicaragua” a conversion of MEKE to both MKE and MEPE: the eddy field loses energy by transferring energy to the mean flow.

The integration of the energy conversion terms for the entire Caribbean Sea in the upper 1000 m depth, summarized in Fig. 6 under the name “CARIBE”, shows that energy is converted from the MKE and MEPE fields into MEKE field. This result suggests that at the scale of the Caribbean Basin, the mean fields transfer energy to the eddy field and not the contrary. Locally, conditions are different. We do not exclude that eddies have an impact on the sCC, by accelerating or decelerating the zonal mean flow and in this way influence its paths. But such interactions are hard to diagnose.

The regional budgets summarized in Fig. 6 might depend on the definition of the regions. To have more confidence on the conclusions previously proposed and for more insight on the geographical differences, terms  $T_2, T_3$  and  $T_4$ , vertically integrated only from 50 to 280 m depth are displayed in Fig. 7. An interesting feature, is the close correspondence of patterns with both  $T_2$  (MEPE  $\rightarrow$  MPE) and  $T_3$  (MEKE  $\rightarrow$  MEPE) negative in Venezuela and Colombia Basins, along the sCC. They are relevant for baroclinic instability processes and are in agreement with the short baroclinic time scale of Fig. 3 and westward growth of MEKE in these regions. A more detailed look allows to identify regions where there is a clear link between enhanced instability (associated with a maximum of energy conversion) and MEKE increase:

- A strong mixed barotropic/baroclinic conversion occurs just west of the Grenada Passage, at  $12^\circ\text{N}$ – $63^\circ\text{W}$ , which has been identified as a region where most of the large Caribbean eddies originate (as illustrated in Section 5).
- The enhancement of baroclinic and barotropic conversion, near  $72^\circ\text{W}$ , after intensification of the sCC by its interaction with the coastline, can be linked with the strong increase of MEKE which occurs in this region (see both model and altimetry MEKE in Fig. 13 of part I).

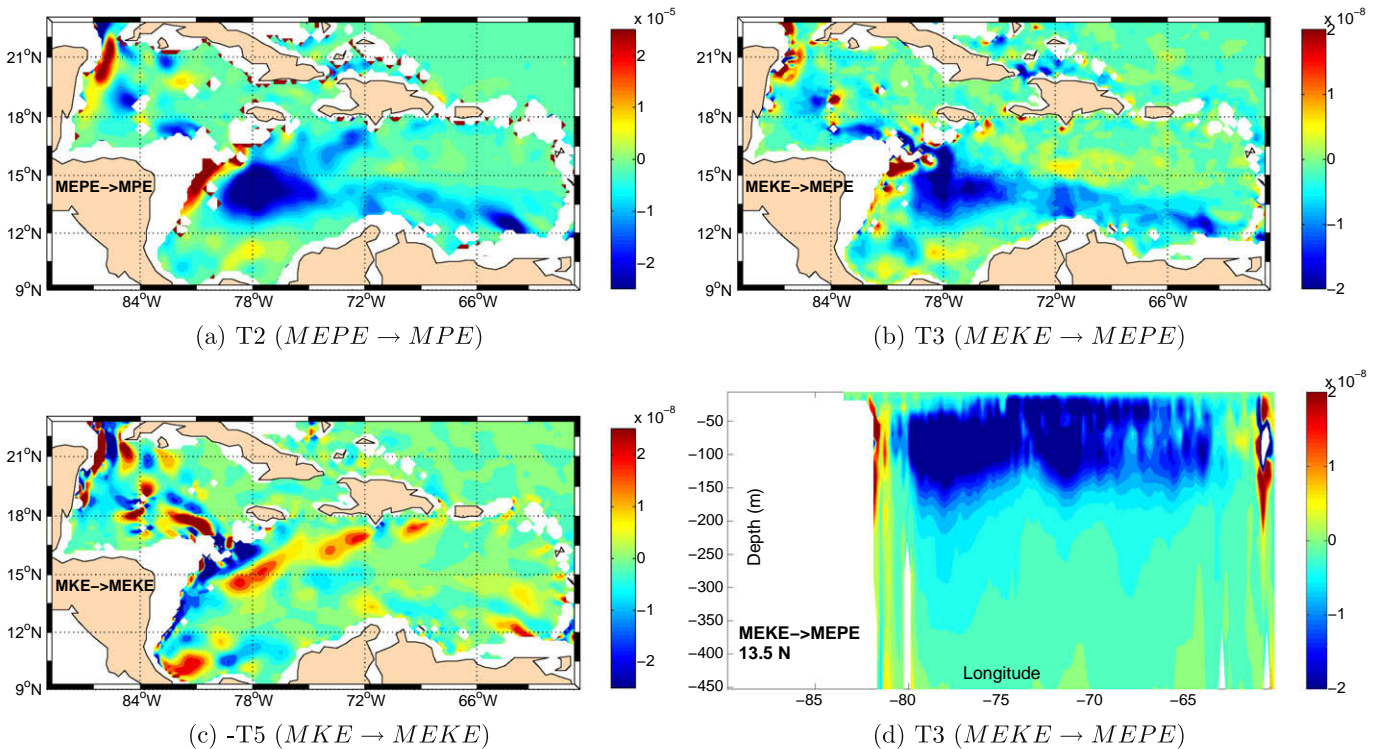


**Fig. 7.** Spatial distribution of energy conversion terms ( $\text{m}^2 \text{ s}^{-3}$ ) (a)  $T_2$  (MEPE  $\rightarrow$  MPE), (b)  $T_3$  (MEKE  $\rightarrow$  MEPE) and (c)  $-T_5$  (MKE  $\rightarrow$  MEKE) averaged from 50 to 280 m depth. Negative values of both  $T_2$  and  $T_3$  are relevant of baroclinic instability process. Positive value of  $T_5$  is relevant of barotropic instability. A vertical section of  $T_3$  (d) at  $13.5^\circ\text{N}$  illustrates that most of the baroclinic energy transfer is done between the surface and 300 m depth.

- A vertical section of  $T_3$  at 13.5°N indicates that the baroclinic conversion occurs mainly in the upper 300 m depth of the sCC (i.e., where the vertical shear of the sCC is significant) and increases westward in the core of the sCC from Venezuela to Colombia Basin. This is fully coherent with a westward growth, deepening and intensification of the eddies along the sCC.

#### 4. The origin of the PV contrast

The sCC constitutes a reservoir of available energy, and part of this energy is released through instability processes to the perturbations. This reservoir has to be recharged or maintained in some way. As explained by Fig. 16 of Jouanno et al. (2008), the sCC belongs to various large scale systems and is fed by: (1) the upper branch of the MOC, as a flux of light water masses (these waters have crossed the equator and were taken to the Lesser Antilles by the Guyana Current and the NBC rings), (2) the deep and wind driven North Atlantic Subtropical Gyre and (3) the NEC. The large scale pressure gradients associated with these large scale circulations maintain the Caribbean mean flow. In addition, the structure of the strong local windstress curl (see Fig. 2) forces a cyclonic circulation in the southern part of the Caribbean Basin and reinforces the anticyclonic circulation in the northern part.

In this section, analysis of the PV fields illustrates how these different current systems fed the sCC and how they cause PV contrasts. It allows to understand why strong PV gradients occur and finally why the mean circulation in the Caribbean Sea is unstable and helps the growth of energetic eddies.

##### 4.1. Calculation of PV

QGPV is calculated following Nakamura and Chao (2001). Their argument to prefer this derivation to the Ertel's PV is that outputs from a geopotential model require vertical interpolations which may cause spurious fluxes and flux divergences of various properties. PV was calculated for both QG and Ertel's derivations. Qualitatively the results are consistent and lead to the same conclusions. Such agreement confirms a posteriori the validity of the QG approximation for this study. We will focus on QGPV for the reasons invoked in Nakamura and Chao (2001) and because PV gradients are better highlighted with this derivation. In practice QGPV is calculated as:

$$\text{QGPV} = f + \zeta + f \frac{\partial \sigma^* / \partial z}{\partial \sigma_0 / \partial z}, \quad (9)$$

where  $f$  is the value of the Coriolis parameter in the Caribbean Sea,  $\zeta$  is the relative vorticity,  $\sigma_0(z)$  the 6 years horizontal mean potential density, and  $\sigma^* = \sigma - \sigma_0$  the anomaly of potential density (Gill, 1982). A useful property of this quantity is its conservation along pressure surfaces in absence of forcing and dissipation. Hence it is well adapted to diagnose outputs from a  $z$ -coordinate model. As recalled by Nakamura and Chao (2001), the stretching term is approximated by the ratio of the perturbation stratification  $\partial \sigma^* / \partial z$  to the reference stratification  $\partial \sigma_0 / \partial z$  and hence represents an anomaly of stretching with respect to a reference stretching for a certain depth. So, when analyzing maps of QGPV calculated with Eq. (9), we should not try to interpret the sign of QGPV since values of QGPV depend on the choice of the reference stratification. But locations of enhanced QGPV gradients and vertical inversion of the sign of QGPV gradients, decisive for questions of instability, are not dependent of the choice of the reference stratification (while sufficiently realist to keep the QG approximation valid) and are well highlighted in this QGPV formulation. Here, the refer-

ence stratification  $\partial \sigma_0 / \partial z$  has been calculated for a domain encompassing the whole Caribbean and part of the North Atlantic (bounded at 50°W).

For all the Caribbean, the stretching term (order  $10^{-5} \text{ s}^{-1}$ ) dominates at each depth the relative vorticity term (order  $10^{-6} \text{ s}^{-1}$ ). But as recalled in Nakamura and Chao (2001), one may not see a greater absolute value of QGPV where  $\partial \sigma^* / \partial z$  is greater, since QGPV depends on how  $\partial \sigma^* / \partial z$  compares with the stratification of the region at the same level. For convenience, we will use the expressions “low QGPV” and “high QGPV” to appoint some patterns in the figures, but be aware that they are not necessarily related with low or high stratification.

##### 4.2. At the origins of the sCC

Meridional sections at 55°W and 62°W in Fig. 8 might help to understand the structure of the Caribbean inflow, decisive to understand why strong  $Q_y$  gradients occur. The section at 55°W shows that the NEC, characterized by a westward flow from 11°N to 15°N, is limited in the model to the upper 200 m depth. Its QGPV (green) contrast with the QGPV of the deep interior flow of the North Atlantic Subtropical Gyre (blue), which flows north of 15°N. As seen in the section at 62°W, the inflow through St. Vincent Passage (mainly a continuation of the NEC) is weaker than the upper flow which enters by the Grenada Passage (mainly a continuation of the Guyana Current). These two contributions merge and form the upper layers of the sCC, whose core can be seen in the section at 71°W. Going back to 62°W, we also identify the contribution from the interior Subtropical Gyre to the Caribbean inflow as various velocity cores which spread between 15°N and 17°N from 70 m depth down to 500 m depth. The organization into various cores is due to the vicinity of the Antilles Passages, located 100–200 km farther east.

At 62°W, the inflow located at 11.5°N and associated with the return flow of the MOC has a QGPV firm which contrasts with the QGPV of the surrounding fluid at the same depth, leading to strong meridional QGPV gradients near the Lesser Antilles. A change of sign of QGPV gradients occurs in many parts of the section, nevertheless we expect that where the currents and the gradients of QGPV are higher (i.e., on the edge of the jet flowing out the Grenada Passage) the instability will result in more energetic eddies. Indeed, larger eddies and higher values of MEKE are found in the southern part of the Caribbean Basin. The snapshots in the following section illustrate that the production of large structures is mainly located near the South American Coast. At 71°W, although the two upper flows have merged, meridional gradients of QGPV change sign in the core of the sCC up to the Nicaraguan Coast, consistent with the high values of baroclinic conversion in the Colombian part of the sCC (as seen in Fig. 7).

More west in the Colombia Basin, QGPV gradients are enhanced by a front between Panama-Colombia Gyre and sCC. Indeed, at 77.6°W the QGPV in the Panama-Colombia Gyre (from 10°N to 14°N) contrasts with the QGPV more north. At 30 m depth in the core of the westward current centered at 14.5°N, strong meridional QGPV gradients occur and are inverted with respect to those which occur at 200 m depth. Note that the westward current corresponds to the sCC, reinforced locally by its convergence with the northern branch of the Panama-Colombia Gyre. The local enhancement of QGPV gradients and of strength of the westward current, explains the strong baroclinic energy conversion calculated in this region, as discussed in Section 3. It suggests that local windstress conditions in the southern Colombia Basin, by driving the dynamics of the Panama-Colombia Gyre, could impact indirectly the growth of the large eddies embedded in the sCC.

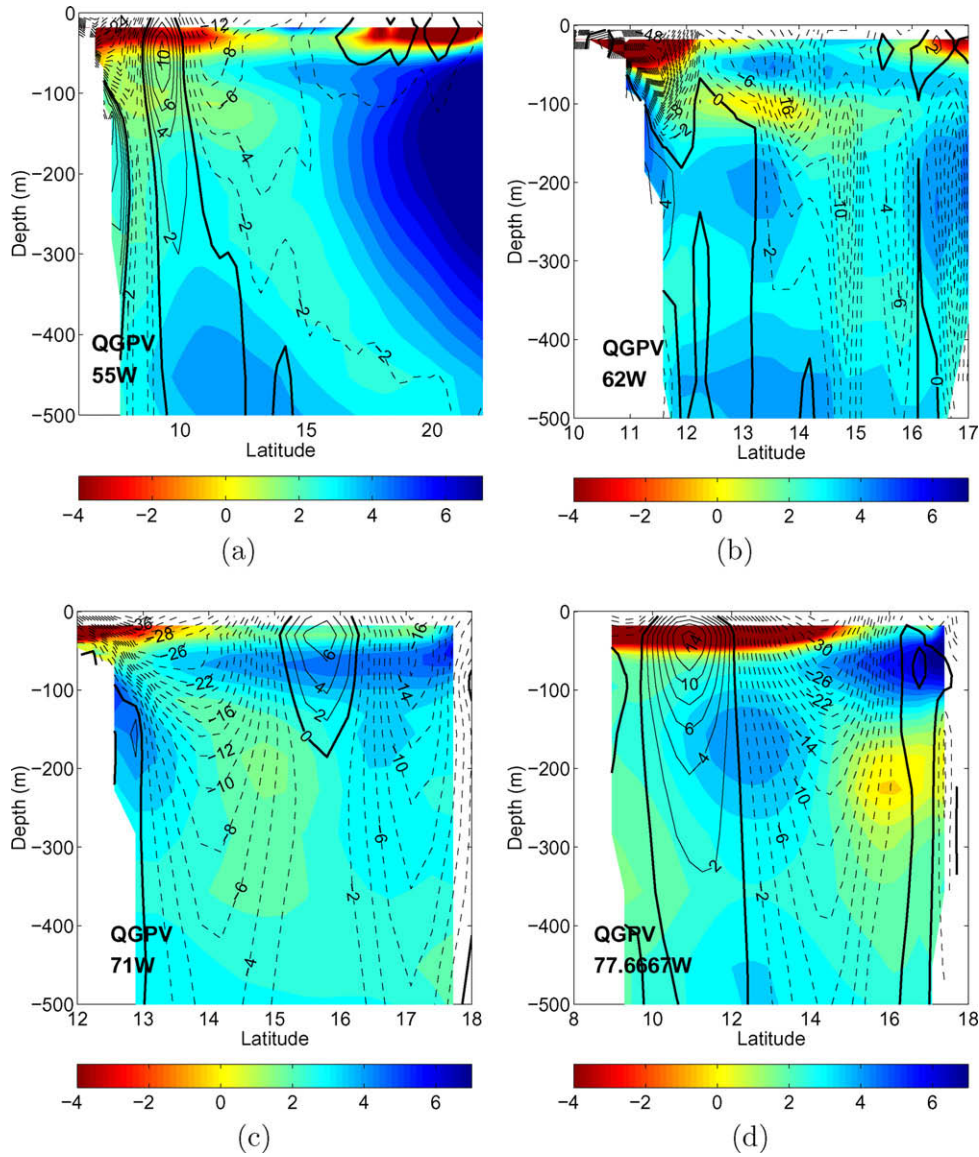


**Fig. 8.** Section of mean QGPV ( $10^{-5} \text{ s}^{-1}$ ; color), calculated with 6 years of data, for the longitudes indicated on the figures. Contours represent the mean zonal velocity ( $\text{m s}^{-1}$ ), with dashed lines as westward velocity and continuous lines as eastward velocity. The reference stratification  $\partial\sigma_0/\partial z$  has been calculated has an horizontal mean of the stratification over a domain encompassing the whole Caribbean and part of the North Atlantic (bounded at  $50^\circ\text{W}$ ).

**5. Formation of the most energetic Caribbean eddies**

Analysis of velocity snapshots and instantaneous QGPV field is illuminating to better understand how the largest Caribbean eddies originate in the eastern Caribbean Sea. Fig. 9 shows snapshots of the QGPV every 20 days at 30 m depth (left column) and 150 m depth (right column). Instantaneous velocity fields at the same depths are superimposed. At day 0, an anticyclone (pattern referenced as A on the figure) and its cyclonic counterpart are growing, respectively, on the northern and southern side of a front characterized by a strong QGPV gradient. Note that at day 0 the flow at 150 m depth near the Grenada Passages (blue color) is oriented eastward, but during the growth of the eddy at day 40, there is an inversion of the flow toward the west. Qualitatively, we can link the flow structure in the region with the Bretherton (1966) interpretation of the two layer baroclinic instability problem in terms of the interaction of two counter propagating Rossby waves (see also Heifetz et al., 2004), and the change of sign of  $Q_y$  in the core of the sCC. Rossby-waves can propagate on a concentrated vorticity

gradient; this process also known as “Rossby-wave quasi elasticity” (e.g., McIntyre GEFD, available at <http://www.atm.damtp.cam.ac.uk/people/mem>). As indicated by the arrow (color magenta) at day 0 in Fig. 9, meridional QGPV gradients in the southern Venezuela Basin are positive at 30 m depth, allowing propagation of quasi-elastic Rossby Waves westward, and negative at 150 m depth, allowing propagation eastward. The growing mechanism proposed by Bretherton (1966) is based on the fact that a layer feels the velocity anomaly (induced by the propagation of a Rossby Wave) produced in the other layer. The relative phase between the counter propagating Rossby Waves tends to lock on a configuration which leads each wave to grow exponentially (see details in Heifetz et al., 2004). This simple two-layer linear theoretical model links eddy growth with strong and localized QGPV gradients.

At day 0, a large NBC ring (A) has traveled northwestward along the Brazilian coast and is reaching the Lesser Antilles. Note how a deep cyclonic circulation (B) blocks the entrance of the Grenada Passage and forces the anticyclone to continue northward. Such



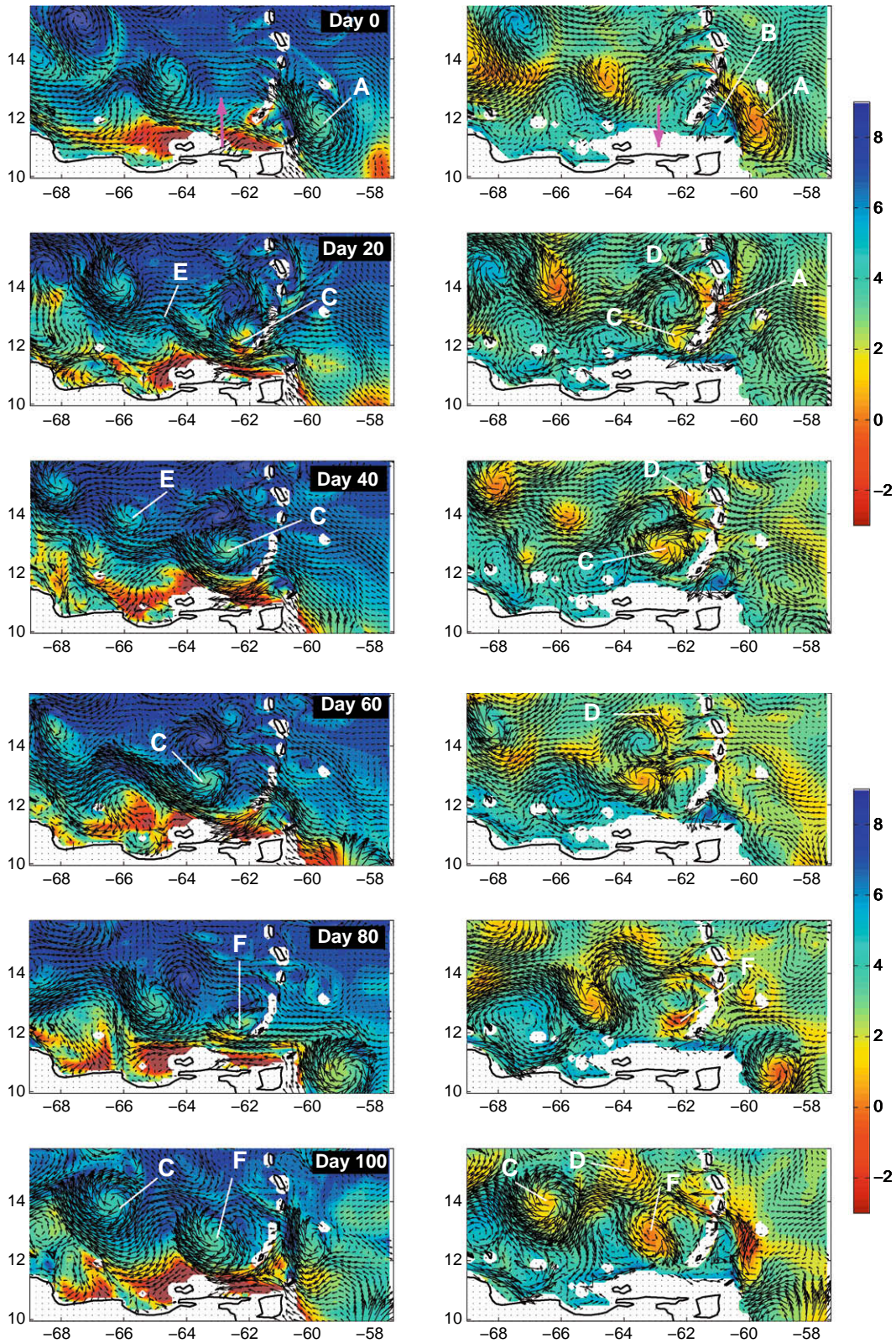


**Fig. 9.** Snapshots of QGPV (color,  $10^{-5} \text{ s}^{-1}$ ) and velocity vectors at 30 m depth (left column) and 150 m depth (right column) for the Antilles-Venezuela region. Each snapshot are separated by 20 days from top to the bottom. The two magenta arrows illustrate the vertical inversion of the QGPV meridional gradients. See text for explanation of letter labels.

behavior is quasi-systematic in the simulation and can also be seen at day 100. At day 20, the anticyclonic ring has lost its structure and gives rise to a circulation around the Lesser Antilles from the

Grenada Passage to the Dominica Passage (clearly seen at 150 m depth). Although the low QGPV core of the ring (A) is entering through St. Vincent Passages, the largest eddy (C) is forming west

of Grenada (located between 300 and 400 km more south than St. Vincent), and a smaller eddy or wave is growing west of St. Vincent (D). These two perturbations appear to be a direct result of the collision of the NBC ring on the Lesser Antilles. The breaking of the ring generates “streamers” or flushes of vorticity anomalies which pass between the islands as suggested by several model studies (Murphy et al., 1999; Barnier et al., 2001). The behavior we have described is well represented by idealized numerical simulations of Simmons and Nof (2002), which studied purely advected eddies through island gaps: in our simulation, the flow presents the characteristics of an eddy encountering a single and elongated barrier (Simmons and Nof (2002) found that the eddy creates a circulation around the island and an anticyclone forms on the southwestern side of the barrier) and an eddy encountering a porous barrier (the eddy creates circulation around the individual island and breaks into various anticyclones).

Although these two perturbations do not appear to be produced by baroclinic instability of the main inflow, their rapid growth might be explained by baroclinic conversion. Note that at day 40, the southern eddy (C) has grown more than the northern eddy (D), this larger growth is consistent with the strong baroclinic conversion which occurs in the southern Venezuela Basin. At day 20, an eddy is forming in a meander of the current (E). This eddy, observable and completely formed 20 days latter, appears to result from the meandering of the main flow. Although the meandering of the main current could be due to the near presence of a ring or to the pure instability of the current, it illustrates that Caribbean mesoscale eddies do not necessarily owe their existence to the advection of vorticity by NBC rings through the Lesser Antilles. Another case of growth can be seen from days 60 to 100: at days 40 and 60, there is no clear eddy pattern east to the Lesser Antilles, but at day 80 an eddy starts to form (F) in the upper layer (there is no trace of it at 150 m depth). At day 100, the eddy is larger and deeper. In this sequence the behavior of the flow at 30 m depth (close to the southern coast and generating many eddies) is very different from the flow at 150 m depth (composed from various inflow sources more to the north, as it can be seen at day 80, and presenting large meanders).

The formation of these two eddies illustrates that large eddies are not systematically produced by entrance or influence of NBC rings. Nevertheless, on the snapshots preceding the formation of the eddies, in both cases the Atlantic westward flow appears to be disturbed, indicating that other kind of perturbations could trigger the baroclinic instability of the mean flow. Although they are not clearly identifiable in the figure, fast Atlantic Rossby waves can pass through the Antilles, as described by Pedlosky (2000). Once inside, these waves can act as finite amplitude perturbations for the baroclinic instability of the mean flow or can interact with eddies. But we will see in the following section that an energetic Caribbean mesoscale variability can be produced in absence of these incoming perturbations.

## 6. Influence of the NBC rings

Results in the previous sections indicate with confidence that the mean Caribbean Currents are unstable and that their instability increases the variability in the Caribbean Basin. It does not mean that instability of the currents drives all the Caribbean mesoscale variability. As mentioned in the introduction, several works link the Caribbean eddy production with NBC rings (e.g., Carton and Chao, 1999; Murphy et al., 1999; Richardson, 2005). In this section, we compare three experiments (NOSLIP, MEAN and VISC; see Table 1 for a description of the experiments) which have different NBC rings and Atlantic eddy/waves production. The analysis shows that in the model, NBC rings or other Atlantic perturbations are not a

necessary condition to set an energetic mesoscale variability in the Caribbean Sea, although they can influence it by acting as finite amplitude perturbations.

Basic statistics highlight the eddy population in the three experiments. In experiment MEAN, the production of surface rings by the NBC retroflection is drastically reduced from 4 or 5 to 1 or 2 eddies shed per year (mainly due to a weakening of the North Equatorial Counter Current; NECC), and therefore less eddies strike the Lesser Antilles. In VISC, all the perturbations coming from the Atlantic are dissipated before reaching the Lesser Antilles and hence there are no more NBC rings or other eddies and waves which enter the Caribbean, coming from the region with artificially enhanced viscosity. Despite this contrast between experiments, the number of large eddies south of Jamaica (4–5 per year) and the number of eddies shed by the Loop Current (1 or 2 per year) is quite similar in the three experiments. A snapshot of the velocity at 30 m depth for VISC experiment is shown in Fig. 10. It illustrates that despite the absence of NBC rings or other Atlantic eddies the Caribbean Sea develops an energetic eddy field.

This result is supported by the integration of MKE and MEKE in the upper 150 m depth for the various basins. We have chosen an integration from the surface to 150 m depth to get more confidence that what we are analyzing is mesoscale turbulence and not only turbulence at the surface. In Table 2, the region “Antilles” is much more energetic in NOSLIP (26) than in MEAN (9.2) or VISC (2.8) due to the occurrence of rings, waves and eddies in the region. Note that in VISC, the lack of mesoscale turbulence benefits the mean flow: MKE is maximum in VISC (14.4). It illustrates that the NBC rings are a mechanism of transport of Equatorial and South Atlantic Water as part of the upper return flow of the MOC (as suggested in Barnier et al., 2001), since in their absence this transport takes a different pathway, namely an enhanced coastal current. Despite these strong differences in the dynamics near the Lesser Antilles, both values of MKE and MEKE for the overall “Caribbean” are very close between each experiment. A look at “Venezuela” or “Colombia” basins shows that MEKE in MEAN or VISC are slightly lower than in NOSLIP, but the difference between experiment is not as strong as for “Antilles”. Moreover, it is difficult to determine exactly whether this weak reduction is associated with the different Atlantic forcing through the Antilles, with a reduction of energy of the mean Caribbean transport or with a change of the main current pathways. Indeed, through a section between Puerto Rico and Venezuela, the  $19.0 \pm 2.3$  Sv of westward transport in the NOSLIP experiment is very near to the  $18.8 \pm 1.9$  Sv in MEAN, but lower than in VISC where it reaches  $23.5 \pm 2.5$  Sv. In conclusion, the drastic differences in variability east of the Lesser Antilles observed comparing the different experiments, do

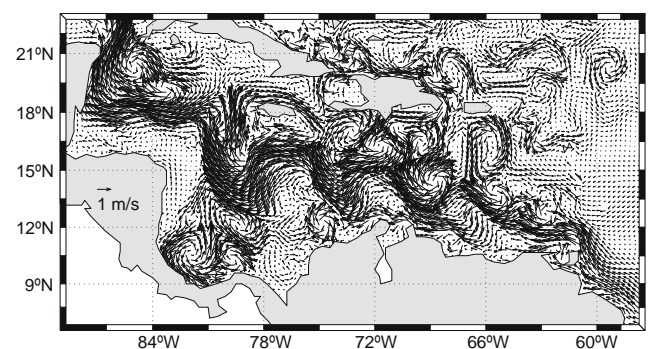


Fig. 10. Instantaneous eddy field in experiment VISC. This snapshot of the velocity at 30 m depth ( $\text{m s}^{-1}$ ) illustrates that without incoming NBC rings an energetic eddy field is produced in the Caribbean Sea. The region over which the Laplacian eddy viscosity has been added is shown in part I.

**Table 2**  
Comparison of MKE and MEKE between the different experiments. For each block, the values are indicated as follows:  $mke (10^{-3} m^2 s^{-2})/meke (10^{-3} m^2 s^{-2})$ . Each MKE and MEKE values correspond to an average over each basin from the surface to 150 m depth. They are calculated from a 6 years mean of kinetic energy and eddy kinetic energy.

Experiment	Caribbean MKE/MEKE	Antilles MKE/MEKE	Venezuela MKE/MEKE	Colombia MKE/MEKE	Cayman MKE/MEKE
NOSLIP	11.7/22.5	10.7/26.0	11.8/20.5	11.3/39.0	27.1/23.7
MEAN	10.0/19.4	8.0/ 9.2	8.1/16.5	8.5/30.4	25.0/14.8
VISC	13.0/20.4	14.4/ 2.8	11.8/16.1	11.3/33.3	32.2/17.9

not produce drastic changes of the eddy field in the interior of the Caribbean Sea.

Variance conserving spectra of SSH for “Atlantic” and “Venezuela” sections are compared in Fig. 11. The “Atlantic” spectra for NOSLIP shows a broad band of variability with periods between 45 and 80 days. The band of periods which ranges between 70 and 75 days is easily explained by the 5 (sometimes 4) anticyclones which reach the Lesser Antilles each year. The broadening of the frequency range (45–80 days<sup>-1</sup>) has two contributions. The first one, is the chaotic behavior of the rings when they collide with the Lesser Antilles, as illustrated by snapshots in Section 5 or by drifter observations (Fratantoni and Richardson, 2006): for example they can split into various eddies, there can be merging among them or they can remain a long time engulfed around the Barbados Island. The second one is the incoming of other perturbations which are not linked to the rings. Indeed, the spectrum for MEAN in Fig. 11 shows a narrow peak centered at 60 days. This period

does not correspond to the NBC eddy shedding, since in this experiment the NBC sheds an average of 1 to 2 eddies per year, but is associated with Rossby waves, as shown as follows.

East of 62°W (i.e., in the Atlantic) in Fig. 12, Hovmoeller diagrams along 14.5°N for NOSLIP and MEAN experiments show perturbations traveling westward. Their wavelengths and westward speed of propagation are respectively  $2\pi/400 km^{-1} < \kappa < 2\pi/550 km^{-1}$  and  $0.07 m s^{-1} < c < 0.1 m s^{-1}$ . We compare these values with the phase speed of first baroclinic mode Rossby waves, whose dispersion relation is given by (e.g., Pedlosky, 1979):

$$\omega = \frac{k(U(k^2 + l^2) - \beta)}{k^2 + l^2 + Ld^{-2}}, \quad (10)$$

where  $\beta = 2.2 \times 10^{-11} m^{-1} s^{-1}$  is the beta parameter at 14.5°N and  $\lambda = 80 km$  is the first mode Rossby radius of deformation calculated in the Caribbean Sea. The value of  $\lambda$  we found is consistent with estimates of Chelton et al. (1998), since they found values ranging from 60 to 80 km in the Caribbean Sea. The speed of the background zonal velocity in the NEC, is estimated with the mean zonal velocity in this region as  $U = 0.05 m s^{-1}$ . This is however a simple theory which does not consider the shear of the main current. Nevertheless several studies show that between 10°N and 30°N this theory is sufficient to match the observed phase speed (e.g., Fu and Chelton, 2000; Colin de Verdière and Tailleux, 2005). Using this dispersion relation, we found that wavelengths from 400 to 500 km are associated with periods between 50 and 65 days. This range of wavelengths is observed in the Hovmoeller diagram, and the Atlantic spectrum for the MEAN experiment gives a peak period centered at 53 days. So, in both experiments Rossby waves with periods near 55 days, impinge on the Lesser Antilles. The origin of such variability is uncertain but could be related to the instability of the NEC. It is remarkable that the frequency of the described Rossby waves ranges is very close to the frequency band of the NBC rings. Although perhaps not surprising, since Jochum and Rizzoli (2003) proposed that NBC surface rings result from the reflection on the Brazilian Coast of Rossby waves produced by the instability of the NECC. Such similitude has an important implication: Rossby waves and NBC rings could act as finite perturbations for instability of the Caribbean Current or force the Caribbean variability in very close ranges of frequencies.

In Fig. 11 for the “Atlantic” section, spectra show an energetic band from 45 to 80 days for NOSLIP which corresponds to the NBC rings and other Atlantic eddies and waves. For MEAN, the band is of weaker amplitude and width and is centered on 53 days, consistent with the period of Rossby waves. In VISC, there is no frequency peak associated with a mesoscale signal. Note that the amplitude of each peak agrees with the respective level of MEKE for “Antilles” in Table 2. Despite the strong differences of the dynamics on the eastern side of the Lesser Antilles, the temporal and spatial scales of the Caribbean mesoscale activity are very close in the three experiments. First, the three spectra along the “Venezuela” section in Fig. 11 show a broad band of variability with peak periods from 50 to 100 days with amplitudes of same order. Second, west of 65°W the three Hovmoeller diagrams in Fig. 12 are similar: meridional velocity values are very close, all show the same zonal wavelength and same speed of propagation.

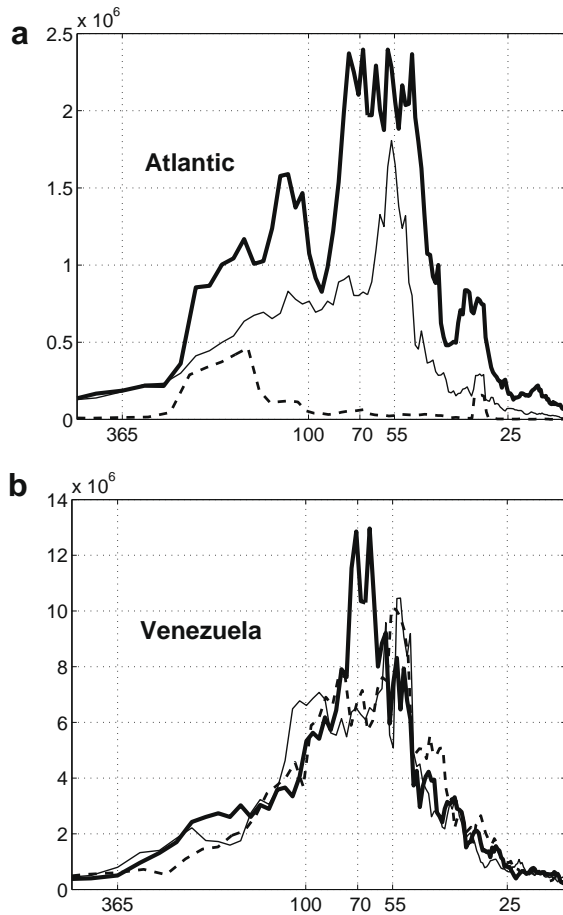


**Fig. 11.** Variance conserving spectrum (Period in day vs  $m^2 \text{ cycle/day}$ ) of SSH calculated for the sections “Atlantic” (57.4°W from 7.5°N to 15.4°N) and “Venezuela” (69.3°W from 11.5°N to 18.6°N) with 6 years of data from NOSLIP (wide line), MEAN (thin line) and VISC (dashed line). The definition of the two sections is the same as for Fig. 15 in part I.

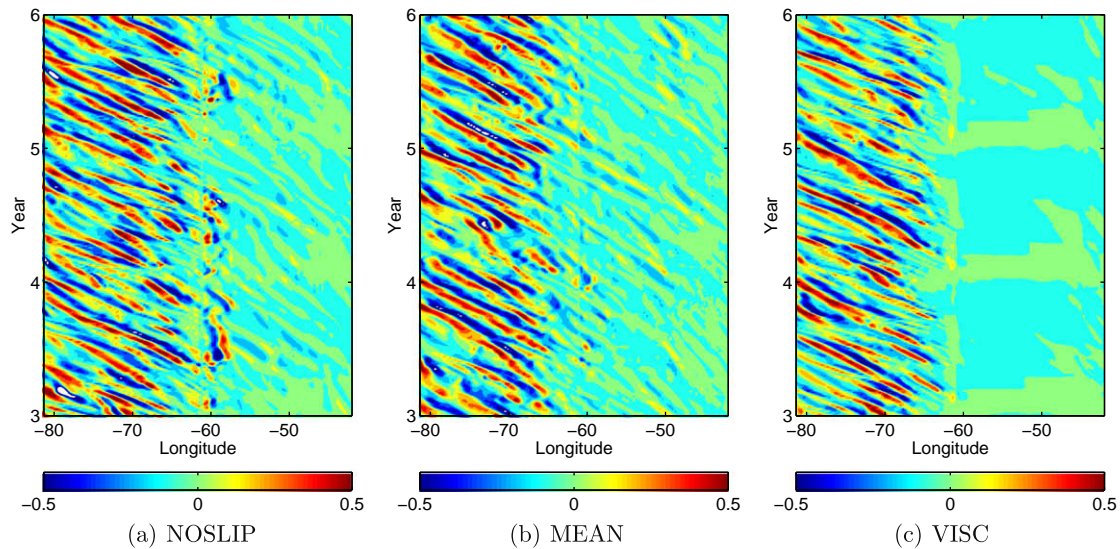


Fig. 12. Hovmoeller diagram calculated with the meridional velocity ( $\text{m s}^{-1}$ ) taken at 50 m depth and  $14.5^\circ\text{N}$ .

In the “Atlantic” spectrum for NOSLIP, there is an energetic variability at 70 days, which we have associated with the advection of NBC rings. The “Atlantic” section is also strongly influenced by the incoming Atlantic Rossby Waves, as indicated by the energetic spectral band which occurs between 50 and 60 days. Now, a careful look at Fig. 11 shows that the spectrum for NOSLIP in “Venezuela” is the only one which presents a significant peak centered at 70 days, whereas both spectra for MEAN and VISC have their maximum near 55 days. VISC indicates that the “natural” frequency of the mesoscale variability for the “Venezuela” section is centered at 55 days. It would mean that the 70 days peak which occurs for NOSLIP in “Venezuela” is linked to the NBC rings: the frequency at which they impinge the Lesser Antilles shifts the formation frequency of the large Caribbean eddies toward lower values.

As a conclusion, the presence or absence of incoming perturbations through the Lesser Antilles do not modify strongly the production of Caribbean eddies. NBC rings are not a necessary condition for the eddy production but since they are present they impact the variability. In particular, they affect the formation frequency of the Caribbean eddies.

## 7. Other regions of eddy production and growth

The eddies embedded in the sCC are the most energetic of the Caribbean Sea, as discussed previously and shown by the high MEKE values in the southern part of the Venezuela and Colombia Basins (Fig. 12 in Jouanno et al., 2008). Out of the sCC pathways, other mesoscale perturbations exist. They are sufficiently strong to impact or dominate the local variability, and are not directly linked with the sCC eddies. In this section, we analyze the dynamics of three regions for which both model and altimetry data show high values of MEKE (see Jouanno et al., 2008): the nCC, the Cayman Current and the Panama–Colombia Gyre. An important result which is highlighted here is the difference in eddy dynamics between different regions.

### 7.1. The northern Caribbean Current

Drifter data of Richardson (2005) and sea level anomaly in Andrade and Barton (2000) show some eddies in the northern part of the Colombia and Venezuela Basins which have entered by the Anageda Passage. The model also produces some small eddies

(<200 km, not shown) south of the Greater Antilles which have been advected from the Atlantic, but others are clearly formed in this region. Oey et al. (2003) report the production of anticyclones south of Hispaniola. They propose that the local and strong anticyclonic windstress curl forces a depression of isopycnals by Ekman pumping and in this way generates large anticyclones. Nevertheless, anticyclones observed with drifters south of Hispaniola in Richardson (2005) started farther east. Richardson results are more consistent with our model, in which anticyclones are advected from the northern Lesser Antilles Passages and cyclones originate on the cyclonic shear of the nCC. In general, the cyclones are rapidly dissipated whereas anticyclones tend to live until merging with larger eddies coming from the southeastern Caribbean.

A careful look in Fig. 3a, reveals a secondary zonal band of short baroclinic time scales just south of Hispaniola, which is indicative of favorable conditions for baroclinic instability of the nCC. The PV analysis shows that in the north of the Colombia section (Fig. 5), both terms change sign and strong gradients of  $Q_y$  occur. Barotropic and baroclinic terms are of same order. Maps of energy conversion terms in Fig. 7 do not provide evidences of baroclinic conversion in the nCC. But such conversion could occur deeper than the integration interval used for the calculation (50–280 m depth). Note that short time scale in Fig. 3 are only seen in the 50–400 m depth average, consistent with the fact that the nCC is deep and has no strong vertical shear in the upper 100 m depth. Nevertheless, the map of barotropic conversion in Fig. 7 shows clearly that the deflection of the nCC near geographic features (mainly south of Hispaniola) allows strong barotropic conversion.

For all these reasons we suggest that barotropic/baroclinic instability of the nCC is the main process responsible for the production of the northern Caribbean eddies. Note the similarity between the nCC in the north of Venezuela and Colombia Basins and the sCC along the South American coast: a coastal and unstable current which can be reached by external perturbations.

### 7.2. The Cayman Current

Although influenced by the circulation in the Colombia Basin, the variability in the Cayman Basin (which also presents a westward growth from the Chibcha Channel) is deeper, less energetic and of lower frequency than the variability in the Colombia and

Venezuela Basins (Jouanno et al., 2008). Our simulations suggest that the strong decrease of MEKE along the Nicaraguan coast in association with an acceleration of the mean flow through the narrow Chibcha Channel allows the Cayman Basin to develop variability with its own particular characteristics.

The “Cayman” section in Fig. 5, shows that the mean zonal flow in this basin is deeper (700 m depth) than the sCC in the “Venezuela” and “Colombia” sections and has a strong horizontal shear down to 500 m depth. In the southern Cayman Basin, the change of  $Q_y$  occurs down to 150 m depth, on the southern and northern edges of the main core, and is dominated by the barotropic term  $\beta - U_{yy}$ . In this region, barotropic instability might be more important than baroclinic instability. Indeed, patterns with both  $T_2$  and  $T_3$  negative in the Cayman Basin occur just west of the Chibcha Channel, although less clear and with lower values than in the Venezuela or Colombia Basins.  $-T_5$  (MKE  $\rightarrow$  MEKE) is maximum and of same order of magnitude as values of  $T_3$  in baroclinically unstable regions such as the Venezuela Basin.

In agreement with the analysis of  $Q_y$ , we conclude that barotropic instability dominates the Cayman Sea. Such difference in generation process can partially explain why the variability produced in the Venezuela and Colombia Basins presents characteristics (depth, structure, frequency) different from the variability found in the Cayman Basin although the events in Cayman cannot be totally disconnected from the upstream variability.

### 7.3. The Panama-Colombia Gyre

The Panama-Colombia Gyre presents a local maximum of variability (MEKE) near the South American Coast, for both altimetry and model data (see Fig. 12 in part I), indicative that local processes enhance the variability in this region. Richardson (2005) mentions some cyclones in this region and suggests three possible mechanisms for their formation which are related to: windstress curl, cyclonic shear of the sCC or temporal separation of pieces of the cyclonic gyre. We propose a fourth hypothesis: the instability of the gyre contributes to the formation and growth of eddies.

Indeed, a band of short baroclinic time scales is found in the southern Colombia Basin, along the Central American coast. It suggests that the eastward flow of the Panama-Colombia Gyre is unstable. Note how the mean current in this region is meandering (Fig. 5 in part I). The eastward flow of the Panama-Colombia Gyre also transfers energy to the eddy field as shown by significant values of baroclinic and barotropic conversion in the southern Colombia Basin (Fig. 7). It confirms that barotropic/baroclinic instability of the Panama-Colombia Gyre can be responsible for the growth of the eddies embedded in it.

## 8. Conclusions

The present work has established a coherent framework for understanding the previously reported heterogeneity of eddy activity and conflicting ideas of eddy generation. It was shown that the instability of the main Caribbean currents is the most relevant explanation for the growth of the mesoscale eddies in the Caribbean Sea. Indeed, any meridional section in the Caribbean Sea satisfies the necessary condition for instability in the quasi-geostrophic approximation, i.e. the meridional gradient of potential vorticity changes sign in the section. This result, although necessary but not sufficient to allow instability, is representative of the dynamical state of the mean flow and its tendency to be unstable. An energy analysis confirms the occurrence of strong energy conversion from the mean currents to the eddy field and hence explains the westward increase of the mean eddy kinetic energy. Calculations reflect strong dynamical differences between basins

within the Caribbean Sea: baroclinic instability dominates the sCC whereas barotropic instability dominates the Cayman Current or the nCC. This result explains why the characteristics of the variability (depth, frequency, energy) in Colombia and Venezuela Basins are different from those in the Cayman Basin, as remarked in part I of this study (Jouanno et al., 2008).

Although instability process can generate eddies all along the Caribbean Sea, we note that in the model most of the large eddies originate near the southern Passages of the Lesser Antilles. Indeed various current systems converge and interact in this region. Flows which include a substantial component of the surface return flow of the MOC (NEC, Guyana Current and NBC rings) merge and enter through Grenada Passage as a shallow and energetic jet with strong vertical and horizontal shears. Hence, most of the energetic eddies in the Venezuela Basin appear to be formed by mixed barotropic/baroclinic instability of this strong inflow. These eddies get rapidly deeper (down to 1000 m depth) and stronger by their interaction with the deep interior flow of the Subtropical Gyre, which enters through passages north to St. Lucia. Subtropical Gyre waters and MOC surface waters merge near 68°W, giving rise to the sCC which is deeper than the Grenada inflow. Nevertheless, the sCC maintains along Venezuela and Colombia basins a strong baroclinic structure which becomes baroclinically unstable and produces the growth of large Caribbean eddies. Note that the Caribbean Coastal Undercurrent, which flows eastward along the continental coast at 200 m depth, contributes to increase the vertical shear of the sCC. The southern Venezuela Basin is among the most unstable regions of the Caribbean Sea and it is also a region where perturbations, due to the interaction of NBC rings with the Lesser Antilles, influence the local variability.

The link between the NBC rings and the Caribbean mesoscale variability can be summarized as follows: NBC rings act as finite perturbations which trigger the instability of the mean flow in the vicinity of the Lesser Antilles. We wish to emphasize the subtlety of this link since results support the idea that the Caribbean Sea is intrinsically unstable and that NBC rings trigger an instability which would occur anyway. Comparison of the results from 3 simulations, which present very different variability west of the Antilles, shows that a cut off of the NBC ring production (and more generally of Atlantic waves and eddies) does not stop the formation of large and energetic Caribbean eddies. Caribbean eddy population or mean eddy kinetic energy are very similar in the different experiments. In the simulation where NBC rings impinge the Lesser Antilles at a period of 70 days, there is a peak of variability in the Venezuela Basin centered at 70 days. When the NBC rings production is cut off, this peak of variability in Venezuela is shifted to 60 days. All this confirms that the main source of energy for the eddy variability in the Caribbean Sea is the instability of the currents, and that the main impact of the NBC rings is to influence the frequency at which the Caribbean eddies are produced.

## Acknowledgements

We acknowledge the provision of supercomputing facilities by the Institut pour le Développement des Ressources en Informatique Scientifique of the Centre National de la Recherche Scientifique, by the Departamento de Supercomputo of the UNAM and by the CICESE (Conacyt project 621-259). Some computations were also performed at Bakliz of DGSCA, UNAM. Altimetry data were produced by Salto/Duacs and distributed by Aviso (<http://www.jason.oceanobs.com>), with support from CNES. The fine grid/coarse grid model configuration was set up in a cooperation between CICESE and the Drakkar project ([www.ifremer.fr/lpo/drakkar](http://www.ifremer.fr/lpo/drakkar)).

## References

- Andrade, C.A., Barton, E.D., 2000. Eddy development and motion in the Caribbean Sea. *Journal of Geophysical Research* 105 (C11), 26191–26201.
- Barnier, S., Reynaud, T., Beckman, A., Boning, C., Molines, J.M., Bernard, S., Jia, Y., 2001. On the seasonal variability and eddies in the North Brazil Current: Insights from model inter-comparison experiments. *Progress in Oceanography* 48, 195–230.
- Beckmann, A., Böning, C.W., Brüggge, B., Stammer, D., 1994. On the generation and role of eddy variability in the central North Atlantic Ocean. *Journal of Geophysical Research* 99 (C10), 20381–20392.
- Bretherton, F.P., 1966. Baroclinic instability and the short wave cut-off in terms of potential vorticity. *Q.J.R. Meteorol. Soc.* 92, 335–345.
- Carton, J.A., Chao, Y., 1999. Caribbean Sea eddies inferred from TOPEX/Poseidon altimetry and a 1/6 Atlantic ocean model circulation. *Journal of Geophysical Research* 104 (C4), 7743–7752.
- Chelton, D., deSzoeke, R., Schlax, M., Naggar, K.E., Siwertz, N., 1998. Geographical variability of the first-baroclinic Rossby radius of deformation. *Journal of Physical Oceanography* 28, 433–460.
- Chérubin, L.M., Richardson, P.L., 2007. Caribbean current variability and the influence of the amazon and orinoco freshwater plumes. *Deep Sea Research I* 54, 1451–1473.
- Colin de Verdière, A., Tailleux, R., 2005. The interaction of a baroclinic mean flow with long Rossby waves. *Journal of Physical Oceanography* 35, 865–879.
- Fratantoni, D.M., Richardson, P.L., 2006. The Evolution and demise of North Brazil Current rings. *Journal of Physical Oceanography* 36, 1241–1264.
- Fratantoni, D.M., Johns, W.E., Townsend, T.L., 1995. Rings of the North Brazil Current: their structure and behaviour inferred from observations and a numerical simulation. *Journal of Geophysical Research* 100 (C6), 10633–10654.
- Fu, L.-L., Chelton, D.B., 2000. Satellite altimetry and earth sciences, Fu, L.L., Cazenave, A. (Eds.), *Large-Scale Ocean Circulation*, vol. 69. International Geophysics Series, pp. 133–169 (Chapter).
- Gill, A.E., 1982. *Atmosphere Ocean Dynamics*. Academic Press.
- Guerrero, L., Sheinbaum, J., Candela, J., 2004. Tracking eddies in the Caribbean Sea using the A VISO altimetry analysis. *Eos, Transactions AGU, Western Pacific Geophysics Meeting Supplement*, 85 (28) (Abstract OS31B-42).
- Heifetz, E., Bishop, C.H., Hoskins, B.J., Methven, J., 2004. The counter-propagating rossby-wave perspective on baroclinic instability. i: Mathematical basis. *Q.J.R. Meteorol. Soc.* 130, 211–231.
- Hernández-Guerra, A., Joyce, T., 2000. Water masses and circulation in the surface layers of the Caribbean at 66°W. *Geophysical Research Letters* 27, 3497–3500.
- Jochum, M., Rizzoli, P.M., 2003. On the generation of North Brazil Current rings. *Journal of Marine Research* 61 (2), 147–173.
- Jouanno, J., Sheinbaum, J., Barnier, B., Molines, J.M., Debreu, L., Lemarié, F., 2008. The mesoscale variability in the caribbean sea. Part I: simulations with an embedded model and characteristics. *Ocean Modell* 23, 82–101.
- Marinone, S., Ripa, P., 1984. Energetics of the instability of a depth independent equatorial jet. *Geophysical Astrophysical Fluid Dynamics* 30, 105–130.
- Masina, S., Philander, S.G.H., 1999. An analysis of tropical instability waves in a numerical model of the Pacific Ocean. 1 Spatial variability of the waves. *Journal of Geophysical Research* 104 (C12), 635.
- Murphy, S.J., Hurlburt, H.E., O'Brien, J.J., 1999. The connectivity of eddy variability in the Caribbean Sea the Gulf of Mexico and the Atlantic Ocean. *Journal of Geophysical Research* 94 (C1), 1431–1453.
- Nakamura, M., Chao, Y., 2001. Diagnoses of an eddy-resolving Atlantic ocean model simulation in the vicinity of the Gulf Stream. Part I: potential vorticity. *Journal of Physical Oceanography* 31, 353–378.
- Oey, L.-Y., Lee, H.-C., Schmitz Jr., W.J., 2003. Effect of winds and Caribbean eddies on the frequency of Loop Current eddy shedding: a numerical model study. *Journal of Geophysical Research* 108 (C10), 3324. doi:10.1029/2002JC001698.
- Pedlosky, J., 1979. *Geophysical Fluid Dynamics*. Springer-Verlag. 624 pp.
- Pedlosky, J., 2000. The transparency of ocean barriers to Rossby waves: the Rossby slit problem. *Journal of Physical Oceanography* 31, 336–352.
- Plumb, R.A., 1983. A new look at the energy cycle. *J. Atmos. Sci.* 40, 1670–1688.
- Richardson, P., 2005. Caribbean Current and eddies as observed by surface drifters. *Deep Sea Research II* 52, 429–463.
- Silander, M., 2005. On the Three-Dimensional structure of Caribbean mesoscale eddies. Thesis of the University of Puerto Rico.
- Simmons, H.F., Nof, D., 2002. The squeezing of eddies through gaps. *Journal of Physical Oceanography* 32, 314–335.
- Talley, L.D., 1983. Radiating instabilities of thin baroclinic jets. *Journal of Physical Oceanography* 13, 2161–2181.
- Tanabe, A., Cenedese, C., 2008. Laboratory experiments on mesoscale vortices colliding with an island chain. *Journal of Geophysical Research* 113 (c4), C04022. doi:10.1029/2007JC004322.
- Tréguier, A.M., Held, I.M., Larichev, V.D., 1997. Parameterization of quasigeostrophic eddies in primitive equation ocean models. *Journal of Physical Oceanography* 27, 567–580.